

High-resolution digital outcrop models of fossil-rifted margins: 3D imaging of extensional detachment systems

Peter Betlem^{1,2*}, Geoffroy Mohn³, Julie Tugend³ and Gianreto Manatschal⁴.

Abstract

Few localities are as important as the outcrops of the remnants of the Alpine Tethys margins exposed in European Alps in the development of new concepts on the temporospatial evolution of magma-poor rifted margins. The Tasna and Err detachment systems are among the best exposed and preserved structures related to extreme crustal thinning and mantle exhumation world-wide. These detachment systems shaped the most distal parts of the fossil Alpine Tethys magma-poor rifted margins and are key analogues of present-day deep-water examples that can only be imaged through geophysical methods. We present the first digitalisation and integration of the Err and Tasna detachment systems using structure-from-motion photogrammetry. The resulting high-resolution models offer details down to 7 cm and cover multi-kilometre cross-sections from various angles. Comparing these 3D digital outcrop models with high-resolution seismic images from the Galicia distal margin allows us to constrain interpretations of the structures and processes that control the formation of distal passive margins. All data are openly available under FAIR (Findable, Accessible, Interoperable, and Reusable) conditions to the geoscientific community, and we hope this contribution will be the first of many that contribute to the ongoing digitalisation of key outcrops of the fossil Alpine Tethys margins in the European Alps.

Introduction

The integration of seismic, borehole and other sub-surface data with outcrop observations is a holistic approach commonly used in the successful exploration of mineral and energy resources. Outcrops bridge seismic and borehole scale observations, provide high-resolution, quantitative constraints, and provide access to unlimited physical and geophysical sampling. In the case of distal rifted margins, buried below thick sediments and/or deep water, access to seismic-scale field analogues provides a unique opportunity to ground truth seismic interpretations. Field analogues enable us to investigate and characterise the complex 3D geometries and fault zone deformations that are fundamental to understand rifting processes and the related fluid flow history. Technological advances over the past two decades have significantly increased the scalability of outcrop analogue studies through the advent of user-friendly mapping tools such as lidar, drones and photogrammetry toolchains [e.g., Marques et al., 2020; Pringle et al., 2006]. At a fraction of the time and cost of traditional methods, it is now possible to swiftly generate correctly scaled and oriented, high-resolution digital outcrop models (DOMs) and seismic-scale digital field sites [e.g., Anell et al., 2016; Westoby et al., 2012]; i.e. digital twins. The acquisition of high-resolution 3D outcrop data is critical for testing and calibrating tectonic models as well as developing new concepts and ascertaining the details of complex geological systems [e.g., Howell et al., 2014].

No longer limited by the ‘local’ nature of single outcrops, geo-referenced representations of multi-outcrop field sites truly bridge the resolution gap from seismic to well data [Marques et al., 2020; Senger et al., 2022]. It is thus unsurprising that DOMs have become the de-facto standard for rigorous outcrop studies, and their importance is evident from the emergence of several key DOM databases [e.g., Betlem et al., In Review; Buckley et al., 2022; Senger et al., 2021]. In addition to providing quantitative data, DOMs provide easy access to otherwise inaccessible areas (e.g., steep cliffs, inhospitable environments) or localities that have since become inaccessible [e.g., Burnham et al., 2022; Senger et al., 2021]. Increasingly, the digital outcrop data sets are made available to the scientific community under FAIR principles [i.e. Findable, Accessible, Interoperable and Reusable; Wilkinson et al., 2016], enabling archiving, temporal studies and reprocessing long after the outcrop is gone [Burnham et al., 2022].

The acquisition and processing of DOMs is well covered in the literature [e.g., Betlem et al., 2022; Betlem and Rodes, 2022; Over et al., 2021; Westoby et al., 2012]. Similarly, there are numerous quantitative data applications, including deciphering the sedimentological and structural evolution and stratigraphic architecture of areas [Corradetti et al., 2018; Tomassetti et al., 2018], and well-documented workflows for follow-up geoscientific processing have been proposed [e.g., de la Varga et al., 2019; Nyberg et al., 2018; Schaaf et al., 2021]. As such, digital

¹ University Centre in Svalbard | ² University of Oslo | ³ CY Cergy Paris Université | ⁴ Université de Strasbourg

* Corresponding author, E-mail: peter.betlem@unis.no

DOI: 10.3997/1365-2397.fb2023032

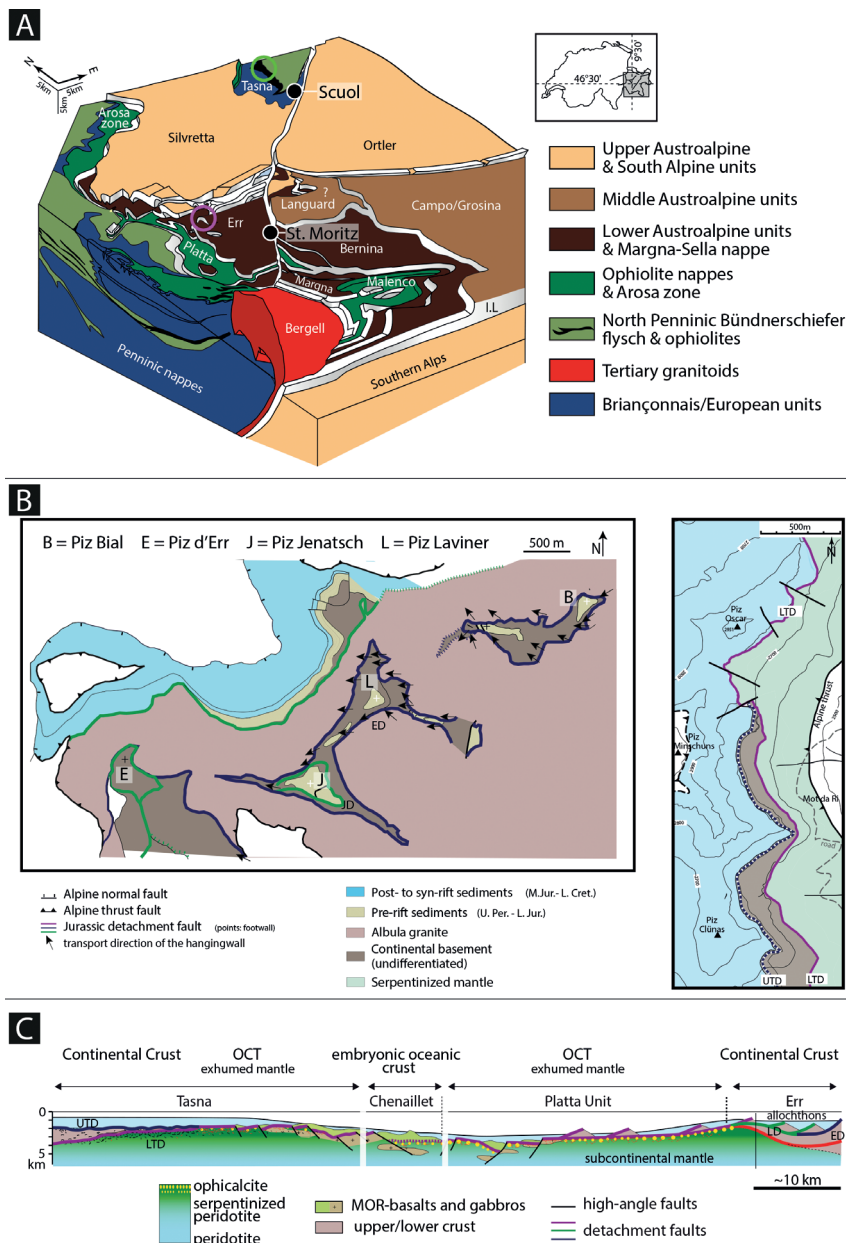


Figure 1 Present-day tectonic position of the Err and Tasna sites in south-eastern Switzerland and main pre-Alpine location of the two sites in the Alpine Tethys margins. A) 3D block showing the Austroalpine and Penninic nappe stack in south-eastern Switzerland and northern Italy ((after Froitzheim et al., [1994]). B) Geological maps of Piz Laviner and Tasna areas after Manatschal and Nievergelt [1997] and Florineth and Froitzheim [1994]. C) Palinspastic reconstruction of the Alpine Tethys margins (modified from Manatschal and Müntener [2009]). Note that the three sites are projected and are not direct conjugate lines.

outcrops represent ideal input data for outcrop-based geo-models [e.g., Enge and Howell, 2010; Howell et al., 2014; Larssen et al., 2020], suitable for e.g. flow simulations [Cabello et al., 2018] and the generation of synthetic seismic images [Anell et al., 2016; Lubrano-Lavadera et al., 2018].

Outcrops preserving remnants of the Alpine Tethys have long played a major role in improving our understanding and in the development of new concepts on the formation and evolution of rifted margins [Lagabrielle and Cannat, 1990; Lemoine et al., 1987; Manatschal et al., 2022; Masini et al., 2013; Mohn et al., 2012; Trümpy, 1975]. Yet, very few – if any – of these unique, kilometre-scale outcrops are digitally documented, let alone as high-resolution, georeferenced DOMs. In this study, we present the first digitalisation and integration of two of the most impressive examples, which are the Err and Tasna detachment systems (Figure 1). Both systems are among the world’s best exposed and preserved examples of detachment systems assumed to shape the most distal parts of present-day, deep-water, magma-poor rifted

margins. The presented outcrops are exceptional in the sense that they preserve the rift-structures and their relation to sediments at a kilometre scale, which makes them perfect for the integration with seismic observations and crucial for understanding modern rift-related detachment systems.

Remnants of the Ancient Tethys Margins

With over a century of scientific publications, the present-day Alpine orogen and former Alpine Tethys rift system are among the best-described tectonic systems in the world [Trümpy, 1975; Lemoine et al., 1987; Mohn et al., 2010; Manatschal et al., 2022]. In particular, the Alps, in south-eastern Switzerland, preserve the remnants of magma-poor rifted margins that were weakly deformed during Alpine orogeny. There, remnants of rift-related structures of the former Jurassic Alpine Tethys are spectacularly exposed (Figure 1), including the Err and Tasna detachment systems.

The Err detachment system is exposed in the Lower Austro-Alpine Err nappe (Figure 1), north of St. Moritz. This

system was first mapped by Froitzheim and Eberli [1990] who interpreted it as Jurassic low-angle detachment faults. Follow-up studies [Manatschal and Nievergelt, 1997; Masini et al., 2011, 2012; Epin and Manatschal, 2018] supported this interpretation and mapped the detachment system over 200 km². Primary pre-Alpine relationships are preserved between Mesozoic pre-, syn-, and post-rift sediments in the hanging wall and exhumed upper crustal granites and gneisses in the footwall (Figure 1). The Err detachment system is interpreted as having formed during the final stage of rifting, related to the exhumation and extreme thinning of the continental crust in the future distal Adriatic margin. A succession of at least three in-sequence detachment faults are now recognised [Epin and Manatschal, 2018], among which the Err and Jenatsch detachment faults shown in our 3D model. These structures are associated with deca-to-kilometre-scale extensional allochthons and Middle Jurassic syn-rift sediments (recognised outside the study area, see Masini et al., [2012]). Reworking of

the characteristic black and green fault rocks within the overlying Middle Jurassic sediments confirms the syn-rift nature of the detachment system [Froitzheim and Eberli, 1990].

The Tasna detachment system is exposed in the Penninic Tasna nappe in the Engadine window north-west of Scuol in south-east Switzerland (Figure 1). Florineth and Froitzheim [1994] were the first to interpret this structure as part of a former Ocean Continent Transition (OCT) of the Briançonnais/European margin of the Alpine Tethys. The outcrop covers a roughly 5 km N-S striking section and exposes exhumed subcontinental mantle that underlies a wedge of thinned mid-to-lower continental crust composed of pre-rift migmatites and Permian gabbros [Florineth and Froitzheim, 1994; Manatschal et al., 2006]. Both the contact separating the crust and the mantle as well as the top of the crust are interpreted as detachment faults, referred to as the Lower and Upper Tasna detachments [Florineth and Froitzheim, 1994]. The Tasna detachment system is sealed by Upper Jurassic to Lower

| Digital model data set | # of images and acquisition parameters | Sparse cloud processing (points) | Dense cloud processing (points) | Mesh processing (faces) | Error X, Y, Z, XY, Total (m, image referencing) | Ground resolution and coverage area |
|-------------------------|--|--|---|---|---|--|
| Tasna detachment system | 1220 | Highest quality: (5816317) RU-filter: 15 (1688942); PA-filter: 3 (1635955); RE-filter: 0.3 (519242) | High quality, mild filtering: (215308830) DCC-filter: 4-255; (115876868) | High quality, dense cloud (17618750) MCCS-filter: 99% (17122113) | 0.126774 m 0.120197 m 0.0484858 m 0.174694 m 0.1813 m | 7.13 cm/pixel; 2.24 km ² |
| Err detachment system | 1082 | Highest quality: (5902134) RU-filter: 15 (2600621); PA-filter: 3 (2409704); RE-filter: 0.3 (927732) | High quality, mild filtering: (598101233) DCC-filter: 5-255; (168743451) | High quality, dense cloud (35665670) MCCS-filter: 99% (35069772) | 0.177225 m 0.144288 m 0.0877425 m 0.228534 m 0.244799 m | 6.82 cm/pixel; 1.96 km ² |

Table 1 Acquisition and processing metadata. RU: reconstruction uncertainty; PA: projection accuracy; RE: reprojection error; DCC: dense cloud confidence; MC: mesh confidence; MCCS: mesh connected component size.

| Data type | Comments | URL/DOI/Reference |
|---|---|--|
| Input imagery and GNSS data | Available for download; including acquisition parameters, and rover/ground station GNSS data. | Tasna detachment system: doi: https://doi.org/10.11582/2023.00003 [Betlem et al., 2023b] Err detachment system: doi: https://doi.org/10.11582/2023.00002 [Betlem et al., 2023a] |
| Data processing project | Available for download; Agisoft Metashape projects and processing reports. | |
| Digital model, orthomosaics, DEM and processing reports | Available for download; Various processing products, including textured mesh in .obj format, orthomosaics in geotiff format, and processing reports- | |
| Digital model (textured) | High-resolution, web-based platform with interpretation possibilities (V3Geo). Data were submitted to V3Geo using the EPSG:32632 coordinate reference system. | Tasna detachment system: https://v3geo.com/model/474 Err detachment system: https://v3geo.com/model/475 |
| Digital model (textured) | Web-based platform with virtual reality integration (SketchFab). | Tasna detachment system: https://sketchfab.com/3d-models/05b270df7e424f7a8c86138aa10ef8c4 Err detachment system: https://sketchfab.com/3d-models/3a19ff2890394f2ba81283c89e1b9d4b |

Table 2 Summary of all data made available to the geoscientific community. Please note that Web-based platforms generally have lesser quality than the downloadable data packages.

Cretaceous deep-marine post-rift sediments, which together with ⁴⁰Ar-³⁹Ar dating on phlogopite and stratigraphic constraints suggest a late Middle to early Late Jurassic exhumation age [Manatschal et al., 2006; Ribes et al., 2020].

Thus, both the Tasna and Err detachment systems formed during the Jurassic opening of the Alpine Tethys, and they provide a unique opportunity to study the processes controlling the separation and final break up of continents in magma-poor settings.

Acquisition and processing

Image acquisition of the Tasna and Err detachment systems was conducted on 9-10 August 2022 using an unmanned aerial vehicle (UAV; Mavic 2 Pro, 20 MP Hasselblad camera) with a TopoDrone post-processed kinematics (PPK) upgrade (L1/L2 GNSS receiver with built-in IMU). Photographs were taken automatically at set time intervals (e.g., 1 photo every 5-10 seconds) in manual flight. All images were manually inspected for quality and, where necessary, provided with masks to cover distal backgrounds and skies. Structure-from-motion photogrammetry processing followed Over et al. [2021] and best practices outlined by the Svalbox project [Betlem et al., In Review].

Data products include high resolution sparse and dense clouds, textured and tiled models, and view-specific orthomosaics.

Table 1 lists the project-specific processing parameters and metadata.

Filtering of the point clouds and mesh introduced few low-point-density areas, mostly affecting out-of-view slopes away from the primary interests. Low-resolution areas observed in the view-specific orthomosaics were replaced with high-resolution textures by manually inserting and assigning specific images to seamlines in Agisoft Metashape. Georeferencing of the outcrops implemented PPK processing using the SwissTopo network, specifically the AGNES stations SAM2 and ARD2, as reference data. The resulting data products are presented in the Swiss national CH1903+ / LV95 (EPSG:2056) projection and are openly available through the links provided in Table 2.

Visualisation, integration and contextualisation

The full data sets, including input imagery and differential GNSS data, processing reports, textured and tiled models, and orthomosaics (as cloud-optimised geotiffs), have been made available under a CreativeCommons BY-NC 4.0 licence, guaranteeing free usability for non-commercial use. The various data products can be visualised and interpreted in both freeware (e.g., Blender [Blender Online Community, 2018], VTK viewers [Schroeder et al., 2006; Sullivan and Kaszynski, 2019], QGIS [QGIS Development Team, 2022]) and subscription services

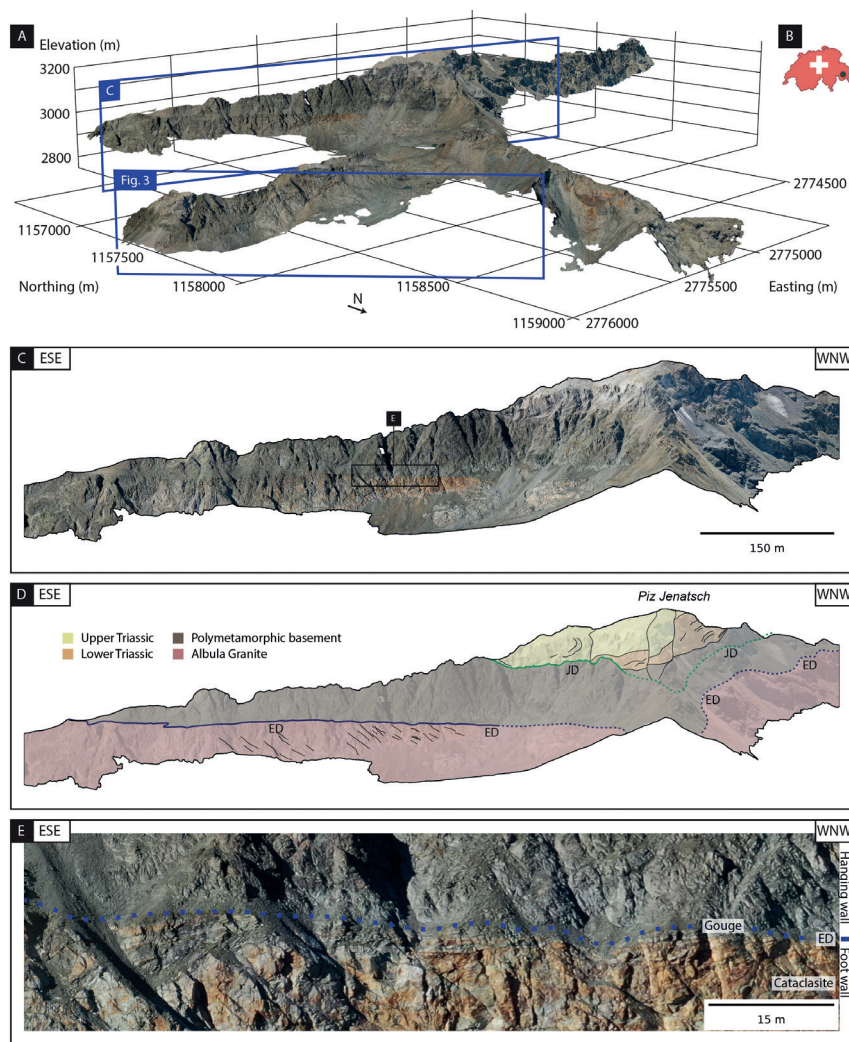


Figure 2 The Err detachment systems exposed at the Piz Laviner distal rifted margin, highlighting A) the extent and quality of the DOM. The inset B) shows the location in Switzerland. The cross-section C) and interpretation D) indicate the main lithostructural elements, including the location of the Err and Jenatsch detachments along the profile. The close-up E) shows the Err detachment, gouge, and cataclases found within the altered Albula Granite (footwall) and polymetamorphic strongly altered basement in the hanging wall. JD: Jenatsch detachment; ED: Err detachment.

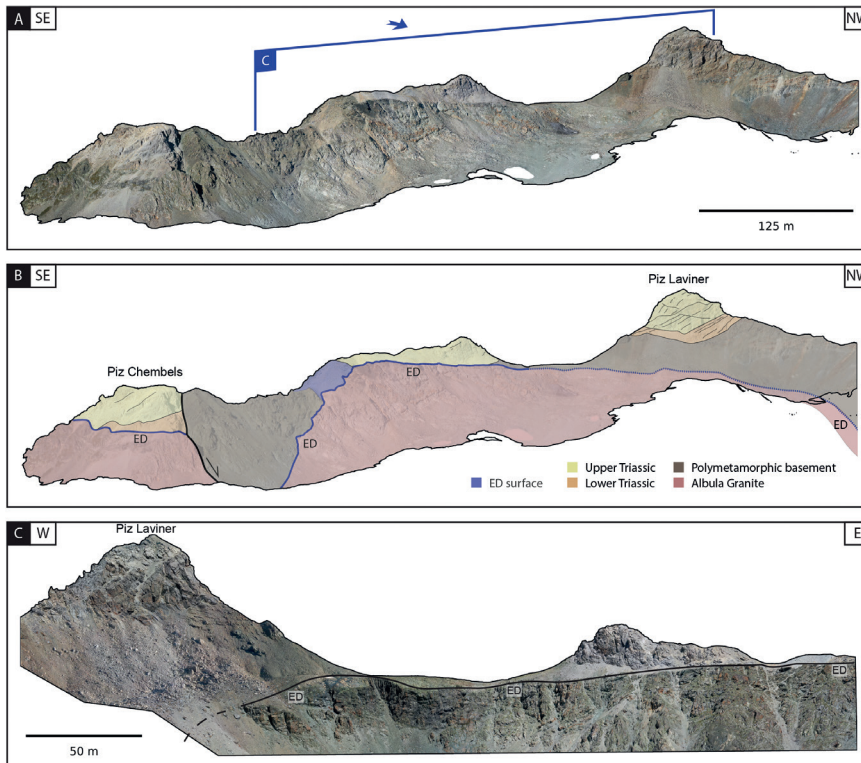


Figure 3 Cross-sections from Piz Chembels to Piz Laviner showing the Err detachment imaged in Figure 2. The south-looking A, B) and north-looking C) cross-sections illustrate the benefits of 3D visualisation in the deciphering of structural complexities. ED: Err detachment.

such as LIME [Buckley et al., 2019] and VRGS [Hodgetts et al., 2015]. The textured models have further been made available as viewable, online resources through V3Geo [Buckley et al., 2022] and SketchFab (Table 2).

With low mean-absolute-position errors and high resolutions (Table 1), the Err and Tasna detachment system DOMs can be directly integrated with existing data sets and literature. The processed outcrop models allow quantitative interpretation of features with details down to the sub-decimetric scale. Veins, fractures, gouges, bedding, and horizons can be readily distinguished in the models (e.g., Figure 2-4), traced in 3D, and used as input for outcrop-constrained geo-models. Though useful on their own, the DOMs are most powerful when integrated directly with other data sets.

The Err Detachment system

The Err detachment system, exposed in the area of Piz Laviner, preserves the 3D rift architecture of the distal Adriatic rifted margin (Figure 2A). The main structural elements are two sub-horizontal detachment surfaces, the Err Detachment (ED) and the Jenatsch Detachment (JD). Both detachments show a top to the W sense of shear (Figures 2 and 3). Epin and Manatschal [2018] interpreted these detachment faults as forming in sequence, with the ED truncated by the JD west of the study area. The footwall of the two detachments correspond to Late Paleozoic granite (i.e., Albula granite) and polymetamorphic basement. The core and damage zones of the detachment faults are several hundred metres thick, with black gouges passing downward to greenish silica-impregnated cataclasites (Figure 2E). The strong, syn-tectonic silica impregnated fault rocks resisted erosion and are the reason why the detachment surfaces are so well expressed morphologically. Geochemistry on fault rocks indicate

the presence of mantle-derived fluids that were channelled along the detachment system and are responsible for the green and red alteration of the footwall and hanging wall rocks [Figure 2E; Pinto et al., 2015].

The ED forms a complex surface, locally cross-cut by late high-angle faults (Figures 3A and 3B). The hanging wall of both the ED and JD is made of extensional allochthons (Figure 3) consisting of polymetamorphic basement and pre-rift Triassic sediments. The relation between the two detachment faults is illustrated in Fig 2 and shows that the JD is laterally located on the hanging wall of the ED. Perhaps the most important observation derived from the DOMs relates to the complex and polyphase deformation history of the hanging wall structures; it predates the final emplacement over the detachment and explains why allochthons cannot be easily restored.

The Tasna Detachment system

The Tasna detachment system, also referred to as the Tasna OCT, is unique in the sense that it exposes the transition from hyper-thinned continental crust to exhumed mantle in a continuous, about 5 km south-north trending outcrop (Figure 4A). This seismic-scale outcrop shows a crustal wedge that is bounded by two detachment faults, the Upper and Lower Tasna detachments (UTD and LTD; Figure 4C and 4D). To the south, the UTD caps continental basement some hundreds of metres thick that spans a complex Palaeozoic to Mesozoic evolution [Froitzheim and Rubatto, 1998; Ribes et al., 2019]. Its footwall comprises a wide damage zone consisting of altered and silica-impregnated continental rocks that show evidence for polyphase brittle faulting. Up-section, the damage zone transitions into gouges, forming the core zone of the detachment, while down-section the LTD forms the contact between the hyper-thinned crust and

the mantle, corresponding to the petrological Moho. Thus far, the cross-cutting relationship between the LTD and UTD remains ambiguous because of their low angle dips. The high resolution and unprecedented perspective provided by the Tasna OCT DOM may be used to ascertain the timing and relationship between the low-angle detachments in future work.

The northern section of the LTD is directly overlain by post-rift Upper Jurassic to Early Cretaceous sediments [Ribes et al., 2019] that are undeformed at the base (Figure 4F), indicating that it was exposed at the seafloor during rifting. The footwall of the LTD is made of serpentinised mantle rocks.

The fault zone of the LTD is several hundred metres thick. It shows a transition from large, rotated and faulted serpentinised mantle blocks that decrease in size up-section and are embedded in a foliated, serpentine and chlorite rich matrix, forming foliated cataclasites and gouges. The top of the exhumed mantle is partly carbonatised [e.g., ophicalcites; Figure 4F; Coltat et al., 2020]. The presence of undeformed sediments over the fault zone of the LTD corroborates the pre-Alpine age of this structure as well as its interpretation as an exhumed detachment.

The Tasna detachment system DOM shows that the LTD is truncated by normal faults with a few metres of offset. The faults are furthermore sealed by the overlying post-rift sediments. The occurrence of two extensional detachment faults affected by high-angle faulting also testifies to the complex polyphase strain evolution of rift-related detachment systems.

Implications for present-day systems

Modern examples of extensional detachment faults are found in the metamorphic core complexes in the SE US Basin and Range

Province [Davis and Lister, 1988; John and Foster, 1993] and from slow spreading Mid Ocean Ridges (MOR) [MacLeod et al., 2009]. The presented digital outcrops are unique since they preserve remnants of rift-related detachment systems that are rarely exposed and preserved elsewhere. The outcrops capture extreme thinning of the continental crust and exhumation of sub-continental mantle, both of which remain less well understood than MOR or post-orogenic extensional systems [Whitney et al., 2013].

Like surface digitalisation methods, subsurface imaging techniques have benefited from technological advances giving increased resolutions. High resolution reflection seismic data have enabled the imaging of structures and their geometrical relationships at present-day distal rifted margins, which are modern examples of the structures observed in the Err and Tasna examples [Figure 5; Gillard et al., 2019; Lymer et al., 2019; Sapin et al., 2021]. Specifically, the Galicia margin (north-west Iberian Peninsula) is commonly interpreted as analogous to the Alpine Tethys [Manatschal, 2004] and benefits from the recent acquisition of a 3D seismic block across its distal margin [Lymer et al., 2019]. Seismic profiles extracted from this 3D block show an array of crustal blocks limited by detachment faults soling out onto the so-called S-reflection [Lymer et al., 2019; Reston et al., 1996].

It is generally accepted that velocities are non-unique [e.g., Karner et al., 2021], leaving significant uncertainty in the interpretation of related lithologies on seismic sections. This is particularly true for distal rifted margins, including exhumed mantle domains, where most rocks have been hydrated and consequently lost their initial rock-properties (e.g., sonic velocity and density). DOMs can be compared directly with the structures and their geometrical relationships observed in seismic sections, either as-is or through

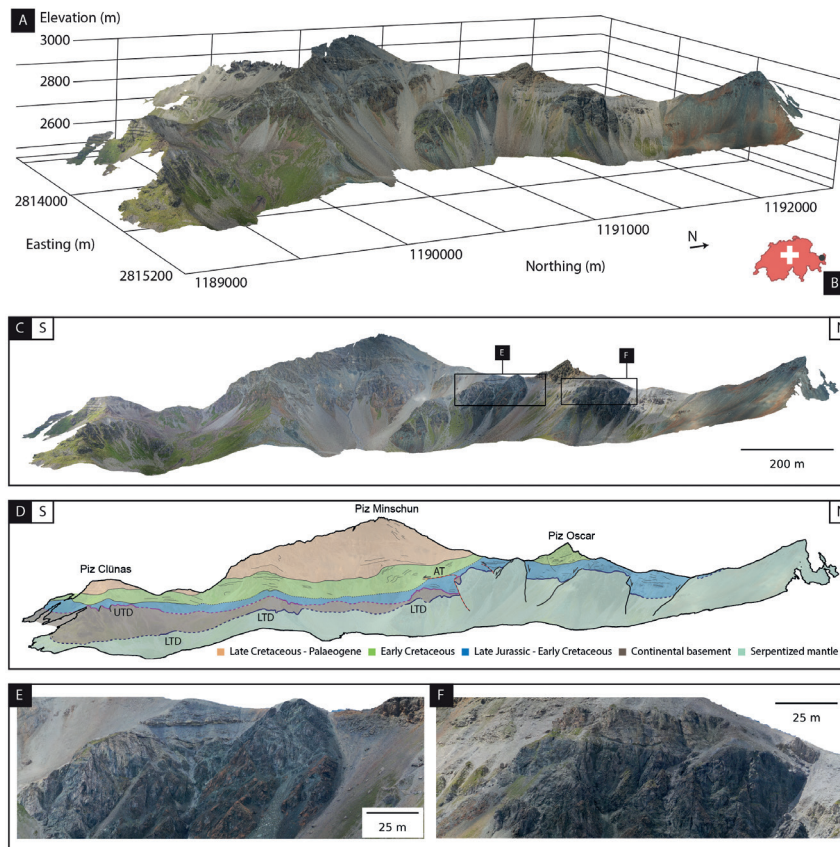


Figure 4 The Tasna detachment system exposed east of Piz Minschun, highlighting A) the extent and quality of the DOM and B) location in Switzerland. The cross-section C) and interpretation D) indicate the main litho-structural elements, including the transition from a hyper-thinned crustal wedge to exhumed mantle along the profile. The close-ups E) and F) illustrate the detail available within the DOMs, including filled veins and fractures in the serpentinized mantle, and the interface between the mantle and sediments. LTD: Lower Tasna detachment; UTD: Upper Tasna detachment; AT: Alpine thrust.

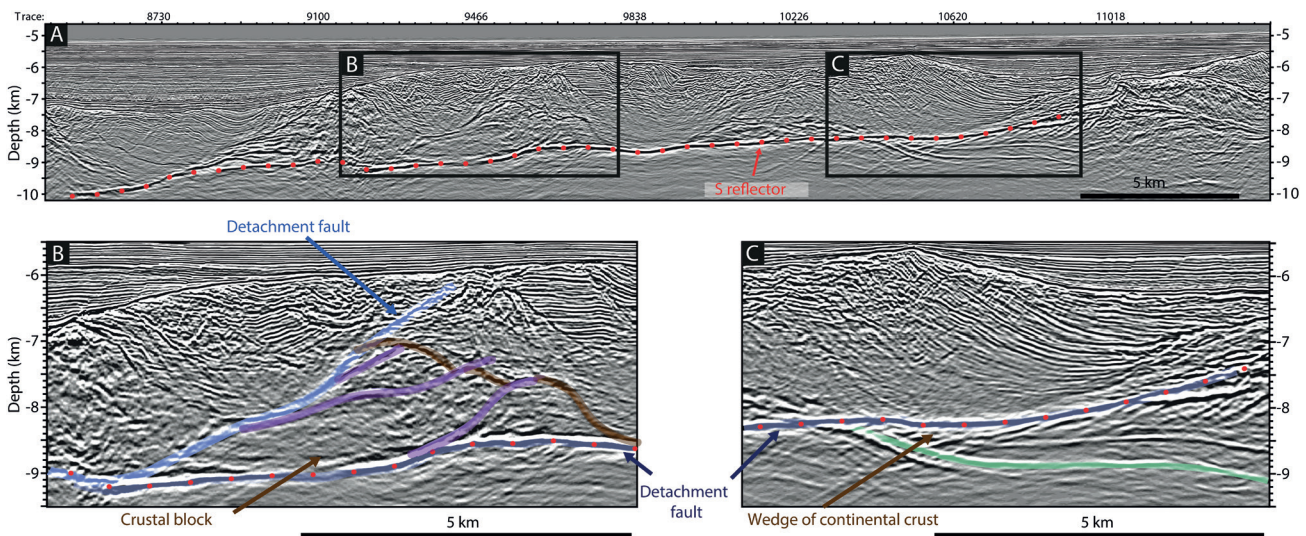


Figure 5 A) Section taken from the 3D seismic block of the Galicia distal margin (north-western Iberian Peninsula, from Lymer et al., [2019]). B) Zoom over a crustal block showing multi-stage extensional faulting. C) Zoom across the continental crust wedge. The Moho reflector is indicated as a green reflector. Modified from Lymer et al., [2019].

seismic modelling. Indeed, Hölker et al. [2002] previously implemented synthetic seismic models of the Tasna OCT to ascertain the tectonic evolution and seismic response of offshore analogs; though their efforts were limited by the low resolution of the geological cross-section available at the time. The very high resolution offered by the DOMs facilitates significantly more complexity in future synthetic models and already provides sub-seismic information on the lithologies and micro-to-meso-scale structural observations. By comparing the DOM data with the Galicia margin seismic data, two main observations can be made:

- 1) Detachment systems show cross-cutting relationships between single detachment faults, as shown in the seismic example in Figure 5A. Figure 5C shows that the S-reflection, interpreted as a composite detachment surface [Lymer et al., 2019], truncates a reflection interpreted as the crust mantle boundary. This situation resembles the crustal wedge observed at Tasna limited by the LTD and UTD (Figure 4).
- 2) Detachment systems are overlain by extensional allochthons or syn-rift sediments (Figure 5B), a situation that is well documented in our digital model data (Figure 2 & 3). High-resolution 3D imaging shows that the extensional allochthons suffered a complex, polyphase, extensional deformation. This setting is comparable to that observed at a larger scale in the 3D seismic images of the Galicia margin where polyphase faulting has been recognised (see Figure 5B; Lymer et al. [2019]).

Detachment systems are thus complex and polyphase 3D structures overlain by deformed allochthon blocks, which makes their restoration challenging.

Conclusion

After more than a century of scientific publications targeting the Alpine Tethys rift system and its evolution, this study is the first to make some of the key outcrops directly accessible to the wider scientific community by using state-of-the-art digitalisation tools. The aim was to present high-resolution DOMs

of detachment systems preserved in the Tasna and Piz Laviner areas in the Alps of SE Switzerland. These outcrops are, to our knowledge, the best exposed examples of detachment systems linked to the extreme thinning of the continental crust and exhumation of sub-continental mantle worldwide. The DOMs show striking similarities to 3D seismic images of present-day magma-poor rifted margins and, in addition, provide information about the lithologies and deformation histories of these systems. The integration of DOMs with multi-physical data, such as high-resolution seismic, is a first yet important step to elucidate the complex structures, geometries, rock types and deformation fabrics of distal margins. Moreover, the DOMs reveal previously inaccessible parts of the system in high detail, resulting in new research questions and paving the way for specific follow-up work on the macroscopic characterisation of such fault zones as well as to test structural models. All data are openly available under FAIR – Findable, Accessible, Interoperable, and Reusable – conditions to the geoscience community, and we hope this contribution will be the first of many that target the digitalisation of the European Alps.

Acknowledgements

We sincerely appreciate the logistical support provided by Helibernina, as well as the educational Metashape licences provided by Agisoft. This study was partly funded by the Norwegian CCS Research Centre (NCCS; industry partners and the Research Council of Norway grant 257579). For the purpose of open access, the author has applied a CC BY public copyright licence to any Author Accepted Manuscript (AAM) version arising from this submission. We thank Kim Senger for fruitful discussions and UNIS and Svalbox for funding PB's participation in the field campaign. We also thank Charlie Kergaravat and Jean-Claude Ringenbach for fruitful discussions during a previous field acquisition and Benjamin Avakian for technical discussions during the 2022 field trip. Finally, we thank Per Terje Osmundsen, an anonymous reviewer and associate editor Angelika Wulff for their constructive feedback on the original submission.

References

- Anell, I., Lecomte, I., Braathen, A. and Buckley, S.J. [2016]. Synthetic seismic illumination of small-scale growth faults, paralic deposits and low-angle clinoforms: A case study of the Triassic successions on Edgeøya, NW Barents Shelf. *Marine and Petroleum Geology*, **77**, 625-639. <https://doi.org/10.1016/j.marpetgeo.2016.07.005>.
- Betlem, P., Birchall, T., Lord, G., Oldfield, S., Nakken, L., Ogata, K. and Senger, K. [2022]. High resolution digital outcrop model of faults and fractures in caprock shales, Konusdalen West, central Spitsbergen. *Earth System Science Data Discussions*, 1-30. <https://doi.org/10.5194/essd-2022-143>.
- Betlem, P., Mohn, G., Tugend, J. and Manatschal, G. [2023a]. *Piz Laviner - Err detachment system digital outcrop data*. <https://doi.org/10.11582/2023.00002>.
- Betlem, P., Mohn, G., Tugend, J. and Manatschal, G. [2023b]. *Piz Minschun - Tasna detachment system digital model data*. <https://doi.org/10.11582/2023.00003>.
- Betlem, P. and Rodes, N. [2022]. *Geo-SfM - Geo-Structure-from-Motion Course: v2022.09.07*. <https://doi.org/10.5281/zenodo.7057605>
- Betlem, P., Rodes, N., Birchall, T., Dahlin, A., Smyrak-Sikora, A. and Senger, K. [In Review]. The Svalbox Digital Model Database: a geoscientific window to the High Arctic. *Geosphere*.
- Blender Online Community [2018]. *Blender - a 3D modelling and rendering package* [Manual]. Retrieved from <http://www.blender.org>.
- Buckley, S.J., Howell, J.A., Naumann, N., Lewis, C., Chmielewska, M., Ringdal, K., ... Pugsley, J. [2022]. V3Geo: a cloud-based repository for virtual 3D models in geoscience. *Geoscience Communication*, **5**(1), 67-82. <https://doi.org/10.5194/gc-5-67-2022>.
- Buckley, S.J., Ringdal, K., Naumann, N., Dolva, B., Kurz, T.H., Howell, J.A. and Dewez, T.J.B. [2019]. LIME: Software for 3-D visualization, interpretation, and communication of virtual geoscience models. *Geosphere*, **15**(1), 222-235. <https://doi.org/10.1130/GES02002.1>.
- Burnham, B.S., Bond, C., Flaig, P.P., van der Kolk, D.A. and Hodgetts, D. [2022]. Outcrop conservation: Promoting accessibility, inclusivity, and reproducibility through digital preservation. *The Sedimentary Record*, **20**(1), 5-14.
- Cabello, P., Domínguez, D., Murillo-López, M.H., López-Blanco, M., García-Sellés, D., Cuevas, J.L., Marzo, M. and Arbués, P. [2018]. From conventional outcrop datasets and digital outcrop models to flow simulation in the Pont de Montanyana point-bar deposits (Ypresian, Southern Pyrenees). *Marine and Petroleum Geology*, **94**, 19-42. <https://doi.org/10.1016/j.marpetgeo.2018.03.040>.
- Coltat, R., Branquet, Y., Gautier, P., Boulvais, P. and Manatschal, G. [2020]. The nature of the interface between basalts and serpentinized mantle in oceanic domains: Insights from a geological section in the Alps. *Tectonophysics*, **797**, 228646. <https://doi.org/10.1016/j.tecto.2020.228646>.
- Corradetti, A., Tavani, S., Parente, M., Iannace, A., Vinci, F., Pirmez, C., ... Mazzoli, S. [2018]. Distribution and arrest of vertical through-going joints in a seismic-scale carbonate platform exposure (Sorrento peninsula, Italy): insights from integrating field survey and digital outcrop model. *Journal of Structural Geology*, **108**, 121-136. <https://doi.org/10.1016/j.jsg.2017.09.009>.
- Davis, G.A. and Lister, G.S. [1988]. Detachment faulting in continental extension; Perspectives from the Southwestern U.S. Cordillera. In S.P. Clark Jr., B.C. Burchfiel, and J. Suppe (Eds.), *Processes in Continental Lithospheric Deformation*, **218**, 0. <https://doi.org/10.1130/SPE218-p133>.
- de la Varga, M., Schaaf, A. and Wellmann, F. [2019]. GemPy 1.0: open-source stochastic geological modeling and inversion. *Geoscientific Model Development*, **12**(1), 1-32. <https://doi.org/10.5194/gmd-12-1-2019>.
- Enge, H.D., and Howell, J.A. [2010]. Impact of deltaic clinoforms on reservoir performance: Dynamic studies of reservoir analogs from the Ferron Sandstone Member and Panther Tongue, Utah. *AAPG Bulletin*, **94**(2), 139-161.
- Epin, M.-E. and Manatschal, G. [2018]. Three-Dimensional Architecture, Structural Evolution, and Role of Inheritance Controlling Detachment Faulting at a Hyperextended Distal Margin: The Example of the Err Detachment System (SE Switzerland). *Tectonics*, **37**(12), 4494-4514. <https://doi.org/10.1029/2018TC005125>.
- Florineth, D. and Froitzheim, N. [1994]. *Transition from continental to oceanic basement in the Tasna Nappe: evidence for Early Cretaceous opening of the Valais Ocean*.
- Froitzheim, N. and Rubatto, D. [1998]. Continental breakup by detachment faulting: field evidence and geochronological constraints (Tasna nappe, Switzerland). *Terra Nova*, **10**(4), 171-176. <https://doi.org/10.1046/j.1365-3121.1998.00187.x>.
- Froitzheim, N., Schmid, S.M. and Conti, P. [1994]. Repeated change from crustal shortening to orogen-parallel extension in the Austroalpine units of Graubünden. *Eclogae Geologicae Helveticae*, **87**(2), 559-612. Retrieved from <http://pascal-francis.inist.fr/vibad/index.php?action=getRecordDetail&idt=4187999>.
- Froitzheim, Nikolaus and Eberli, G.P. [1990]. Extensional detachment faulting in the evolution of a Tethys passive continental margin, Eastern Alps, Switzerland. *GSA Bulletin*, **102**(9), 1297-1308. [https://doi.org/10.1130/0016-7606\(1990\)102<1297:EDFITE>2.3.CO;2](https://doi.org/10.1130/0016-7606(1990)102<1297:EDFITE>2.3.CO;2).
- Gillard, M., Tugend, J., Müntener, O., Manatschal, G., Karner, G.D., Autin, J., Sauter, D., Figueredo, P. H. and Ulrich, M. [2019]. The role of serpentinization and magmatism in the formation of decoupling interfaces at magma-poor rifted margins. *Earth-Science Reviews*, **196**, 102882. <https://doi.org/10.1016/j.earscirev.2019.102882>.
- Hodgetts, D., Seers, T., Head, W., and Burnham, B. S. [2015]. *High Performance Visualisation of Multiscale Geological Outcrop Data in Single Software Environment*. 2015(1), 1-5. <https://doi.org/10.3997/2214-4609.201412862>
- Hölker, A.B., Manatschal, G., Holliger, K. and Bernoulli, D. [2002]. Seismic structure and response of ocean-continent transition zones – A comparison of an ancient Tethyan and a present-day Iberian site. *Marine Geophysical Researches*, **23**(4), 319-334. <https://doi.org/10.1023/A:1025706125747>.
- Howell, J.A., Martinius, A.W. and Good, T.R. [2014]. The application of outcrop analogues in geological modelling: a review, present status and future outlook. *Geological Society, London, Special Publications*, **387**(1), 1-25. <https://doi.org/10.1144/SP387.12>.
- John, B.E. and Foster, D.A. [1993]. Structural and thermal constraints on the initiation angle of detachment faulting in the southern Basin and Range: The Chemehuevi Mountains case study. *GSA Bulletin*, **105**(8), 1091-1108. [https://doi.org/10.1130/0016-7606\(1993\)105<1091:SATCOT>2.3.CO;2](https://doi.org/10.1130/0016-7606(1993)105<1091:SATCOT>2.3.CO;2).
- Karner, G.D., Johnson, C., Shoffner, J., Lawson, M., Sullivan, M., Sitgreaves, J., McHarge, J., Stewart, J. and Figueredo, P. [2021]. *Chapter 9: Tectono-Magmatic Development of the Santos and Campos Basins, Offshore Brazil*. 215-256. <https://doi.org/10.1306/13722321MSB.9.1853>.

- Lagabriele, Y. and Cannat, M. [1990]. Alpine Jurassic ophiolites resemble the modern central Atlantic basement. *Geology*, **18**(4), 319-322. [https://doi.org/10.1130/0091-7613\(1990\)018<0319:AJORTM>2.3.CO;2](https://doi.org/10.1130/0091-7613(1990)018<0319:AJORTM>2.3.CO;2).
- Larsen, K., Senger, K. and Grundvåg, S.-A. [2020]. Fracture characterization in Upper Permian carbonates in Spitsbergen: A workflow from digital outcrop to geo-model. *Marine and Petroleum Geology*, **122**, 104703. <https://doi.org/10.1016/j.marpetgeo.2020.104703>.
- Lemoine, M., Tricart, P., and Boillot, G. [1987]. Ultramafic and gabbroic ocean floor of the Ligurian Tethys (Alps, Corsica, Apennines): In search of a genetic model. *Geology*, **15**(7), 622-625. [https://doi.org/10.1130/0091-7613\(1987\)15<622:UAGOFO>2.0.CO;2](https://doi.org/10.1130/0091-7613(1987)15<622:UAGOFO>2.0.CO;2).
- Lubrano-Lavadera, P., Senger, K., Lecomte, I., Mulrooney, M.J. and Kühn, D. [2018]. Seismic modelling of metre-scale normal faults at a reservoir-cap rock interface in Central Spitsbergen, Svalbard: implications for CO₂ storage. *Norwegian Journal of Geology*. <https://doi.org/10.17850/njg003>.
- Lymer, G., Cresswell, D.J.F., Reston, T.J., Bull, J.M., Sawyer, D.S., Morgan, J.K., ... Shillington, D.J. [2019]. 3D development of detachment faulting during continental breakup. *Earth and Planetary Science Letters*, **515**, 90-99. <https://doi.org/10.1016/j.epsl.2019.03.018>.
- MacLeod, C.J., Searle, R.C., Murton, B.J., Casey, J.F., Mallows, C., Unsworth, S.C., Achenbach, K.L. and Harris, M. [2009]. Life cycle of oceanic core complexes. *Earth and Planetary Science Letters*, **287**(3), 333-344. <https://doi.org/10.1016/j.epsl.2009.08.016>.
- Manatschal, G. [2004]. New models for evolution of magma-poor rifted margins based on a review of data and concepts from West Iberia and the Alps. *International Journal of Earth Sciences*, **93**(3), 432-466. <https://doi.org/10.1007/s00531-004-0394-7>.
- Manatschal, G., Chenin, P., Ghienne, J.-F., Ribes, C. and Masini, E. [2022]. The syn-rift tectono-stratigraphic record of rifted margins (Part I): Insights from the Alpine Tethys. *Basin Research*, **34**(1), 457-488. <https://doi.org/10.1111/bre.12627>.
- Manatschal, G., Engström, A., Desmurs, L., Schaltegger, U., Cosca, M., Müntener, O. and Bernoulli, D. [2006]. What is the tectono-metamorphic evolution of continental break-up: The example of the Tasna Ocean-Continent Transition. *Journal of Structural Geology*, **28**(10), 1849-1869. <https://doi.org/10.1016/j.jsg.2006.07.014>.
- Manatschal, G. and Müntener, O. [2009]. A type sequence across an ancient magma-poor ocean-continent transition: the example of the western Alpine Tethys ophiolites. *Tectonophysics*, **473**(1), 4-19. <https://doi.org/10.1016/j.tecto.2008.07.021>.
- Manatschal, G. and Nievergelt, P. [1997]. A continent-ocean transition recorded in the Err and Platta nappes (Eastern Switzerland). *Eclogae Geologicae Helveticae*, **90**(1), 3-28.
- Marques, A., Horota, R.K., de Souza, E.M., Kupssinskü, L., Rossa, P., Aires, A.S., ... Cazarin, C.L. [2020]. Virtual and digital outcrops in the petroleum industry: A systematic review. *Earth-Science Reviews*, **208**, 103260. <https://doi.org/10.1016/j.earscirev.2020.103260>.
- Masini, E., Manatschal, G. and Mohn, G. [2013]. The Alpine Tethys rifted margins: Reconciling old and new ideas to understand the stratigraphic architecture of magma-poor rifted margins. *Sedimentology*, **60**(1), 174-196. <https://doi.org/10.1111/sed.12017>.
- Masini, E., Manatschal, G., Mohn, G., Ghienne, J.-F. and Lafont, F. [2011]. The tectono-sedimentary evolution of a supra-detachment rift basin at a deep-water magma-poor rifted margin: the example of the Samedan Basin preserved in the Err nappe in SE Switzerland. *Basin Research*, **23**(6), 652-677. <https://doi.org/10.1111/j.1365-2117.2011.00509.x>.
- Masini, E., Manatschal, G., Mohn, G. and Unternehr, P. [2012]. Anatomy and tectono-sedimentary evolution of a rift-related detachment system: The example of the Err detachment (central Alps, SE Switzerland). *GSA Bulletin*, **124**(9-10), 1535-1551. <https://doi.org/10.1130/B30557.1>.
- Mohn, G., Manatschal, G., Beltrando, M., Masini, E. and Kusznir, N. [2012]. Necking of continental crust in magma-poor rifted margins: Evidence from the fossil Alpine Tethys margins. *Tectonics*, **31**(1). <https://doi.org/10.1029/2011TC002961>.
- Mohn, Manatschal, G., Müntener, O., Beltrando, M. and Masini, E. [2010]. Unravelling the interaction between tectonic and sedimentary processes during lithospheric thinning in the Alpine Tethys margins. *International Journal of Earth Sciences*, **99**(1), 75-101. <https://doi.org/10.1007/s00531-010-0566-6>.
- Nyberg, B., Nixon, C.W. and Sanderson, D.J. [2018]. NetworkGT: A GIS tool for geometric and topological analysis of two-dimensional fracture networks. *Geosphere*, **14**(4), 1618-1634. <https://doi.org/10.1130/GES01595.1>.
- Over, J.-S.R., Ritchie, A.C., Kranenburg, C.J., Brown, J.A., Buscombe, D.D., Noble, T., Sherwood, C.R., Warrick, J.A. and Wernette, P.A. [2021]. *Processing coastal imagery with Agisoft Metashape Professional Edition, version 1.6—Structure from motion workflow documentation*. US Geological Survey.
- Pinto, V.H.G., Manatschal, G., Karpoff, A.M. and Viana, A. [2015]. Tracing mantle-reacted fluids in magma-poor rifted margins: The example of Alpine Tethyan rifted margins. *Geochemistry, Geophysics, Geosystems*, **16**(9), 3271-3308. <https://doi.org/10.1002/2015GC005830>.
- Pringle, J.K., Howell, J.A., Hodgetts, D., Westerman, A.R., and Hodgson, D.M. [2006]. Virtual outcrop models of petroleum reservoir analogues: a review of the current state-of-the-art. *First Break*, **24**(3). <https://doi.org/10.3997/1365-2397.2006005>.
- QGIS Development Team. [2022]. *QGIS geographic information system [Manual]*. Retrieved from <https://www.qgis.org>.
- Reston, T.J., Krawczyk, C.M. and Klaeschen, D. [1996]. The S reflector west of Galicia (Spain): Evidence from prestack depth migration for detachment faulting during continental breakup. *Journal of Geophysical Research: Solid Earth*, **101**(B4), 8075-8091. <https://doi.org/10.1029/95JB03466>.
- Ribes, C., Ghienne, J.-F., Manatschal, G., Decarlis, A., Karner, G.D., Figueredo, P.H., and Johnson, C.A. [2019]. Long-lived mega fault-scarps and related breccias at distal rifted margins: insights from present-day and fossil analogues. *Journal of the Geological Society*, **176**(5), 801-816. <https://doi.org/10.1144/jgs2018-181>.
- Ribes, C., Petri, B., Ghienne, J.-F., Manatschal, G., Galster, F., Karner, G.D., Figueredo, P.H., Johnson, C.A. and Karpoff, A.-M. [2020]. Tectono-sedimentary evolution of a fossil ocean-continent transition: Tasna nappe, central Alps (SE Switzerland). *GSA Bulletin*, **132**(7-8), 1427-1446. <https://doi.org/10.1130/B35310.1>.
- Sapin, F., Ringenbach, J.-C. and Clerc, C. [2021]. Rifted margins classification and forcing parameters. *Scientific Reports*, **11**(1), 8199. <https://doi.org/10.1038/s41598-021-87648-3>.
- Schaaf, A., de la Varga, M., Wellmann, F. and Bond, C.E. [2021]. Constraining stochastic 3-D structural geological models with topology information using approximate Bayesian computation in GemPy 2.1. *Geoscientific Model Development*, **14**(6), 3899-3913. <https://doi.org/10.5194/gmd-14-3899-2021>.
- Schroeder, W., Martin, K. and Lorensen, B. [2006]. *The visualization toolkit*, 4th edn. Kitware. New York.

- Senger, K., Betlem, P., Birchall, T., Buckley, S.J., Coakley, B., Eide, C.H., ... Smyrak-Sikora, A. [2021]. Using digital outcrops to make the high Arctic more accessible through the Svalbox database. *Journal of Geoscience Education*, **69**(2), 123-137. <https://doi.org/10.1080/10899995.2020.1813865>.
- Senger, K., Betlem, P., Birchall, T., Jr, L.G., Grundvåg, S.-A., Horota, R.K., ... Smyrak-Sikora, A. [2022]. Digitising Svalbard's Geology: the Festningen Digital Outcrop Model. *First Break*, **40**(3), 47-55. <https://doi.org/10.3997/1365-2397.fb2022021>.
- Sullivan, C.B. and Kaszynski, A.A. [2019]. PyVista: 3D plotting and mesh analysis through a streamlined interface for the Visualization Toolkit (VTK). *Journal of Open Source Software*, **4**(37), 1450. <https://doi.org/10.21105/joss.01450>.
- Tomassetti, L., Petracchini, L., Brandano, M., Trippetta, F. and Tomassi, A. [2018]. Modeling lateral facies heterogeneity of an upper Oligocene carbonate ramp (Salento, southern Italy). *Marine and Petroleum Geology*, **96**, 254-270. <https://doi.org/10.1016/j.marpetgeo.2018.06.004>.
- Trümpy, R. [1975]. Penninic-Austroalpine boundary in the Swiss Alps: a presumed former continental margin and its problems. *American Journal of Science*, **275**(A), 209-238.
- Westoby, M.J., Brasington, J., Glasser, N.F., Hambrey, M.J. and Reynolds, J.M. [2012]. 'Structure-from-Motion' photogrammetry: A low-cost, effective tool for geoscience applications. *Geomorphology*, **179**, 300-314. <https://doi.org/10.1016/j.geomorph.2012.08.021>.
- Whitney, D. L., Teyssier, C., Rey, P., and Buck, W. R. [2013]. Continental and oceanic core complexes. *GSA Bulletin*, **125**(3-4), 273-298. <https://doi.org/10.1130/B30754.1>.
- Wilkinson, M.D., Dumontier, M., Aalbersberg, Ij. J., Appleton, G., Axton, M., Baak, A., ... Mons, B. [2016]. The FAIR Guiding Principles for scientific data management and stewardship. *Scientific Data*, **3**(1), 160018. <https://doi.org/10.1038/sdata.2016.18>.